

Summary: EXS, EXW, ICC

Abhijit Sen



25th IAEA Fusion Energy Conference

St. Petersburg, 13-18 October, 2014

Thanks to all authors and overview speakers who sent slides
Special thanks to C. Greenfield, P. Kaw, H. Yamada

Outline

Topic	Number of Papers
Magnetic Confinement Expts: Stability (EXS)	56
Magnetic Confinement Expts: Waves (EXW)	54
Innovative Confinement Concepts (ICC)	15

Subtopics for EXS & EXW (guided by ITER priority needs)

- **Disruptions/Runaways** (control, mitigation, prediction)
- **ELMS** (control, mitigation) & **3D physics**
- **Waves and Energetic Particles**
- **MHD instabilities (nonlinear interactions, control)**
- **Current Drive & RF Heating**

Disruptions / Runaways – a major concern for ITER operation

EX/P3-18, Campbell

Main Issues

- Uncertainties associated with disruption loads that can impact the structural integrity of the machine
- How to limit the number of disruptions to protect machine life
 - Disruption avoidance /control
 - Disruption prediction
- Need for a reliable disruption mitigation system (thermal, current and runaway mitigation) – input required before final design review 2017
- Many gaps in physics basis and a lack of fundamental understanding

Disruption Research has Increased and Become More Focused since the 2012 FEC

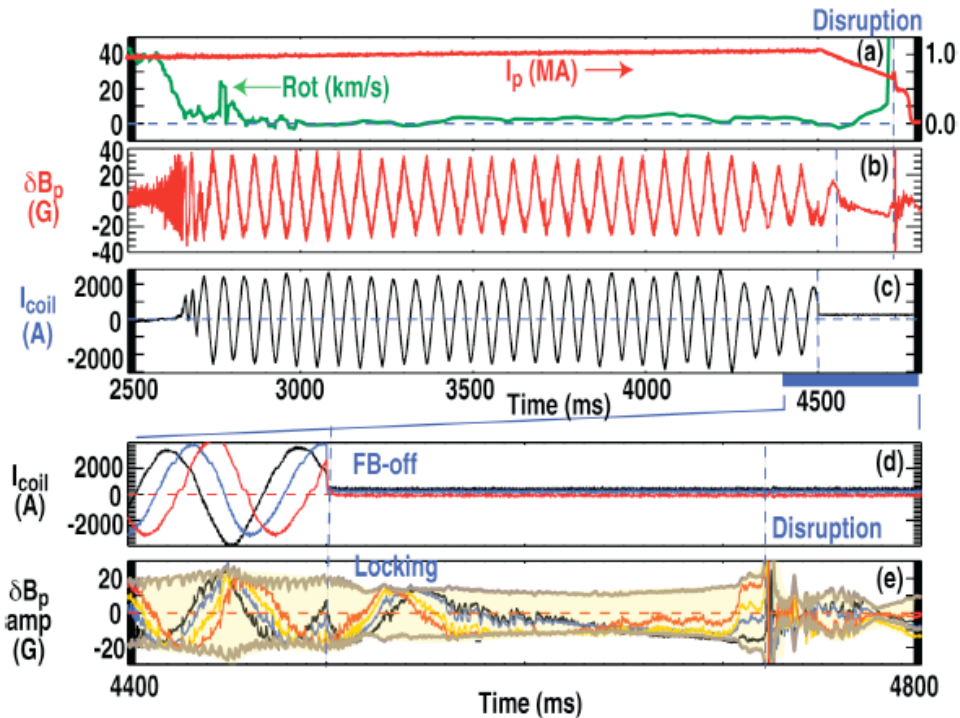
- **Prediction and avoidance**
 - ✓ Both empirical and theory-based
 - Halo currents – measurements and modeling
 - ✓ Exploration of various techniques for disruption avoidance
- **Characterization**
 - ✓ **Enlarged experimental database + modeling has led to improved understanding**
 - ✓ Asymmetric events – causes and consequences
- **Mitigation and control**
 - ✓ Thermal/current quench mitigation experiments
 - ✓ Runaway generation and control

ITPA has played a major role in coordinating and contributing towards joint experimental + modeling activities

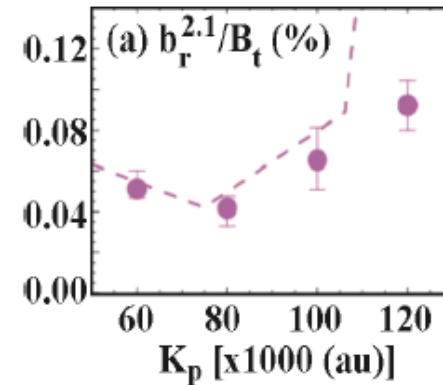
Disruption Avoidance / Control

EX/P2-42, Okabayashi

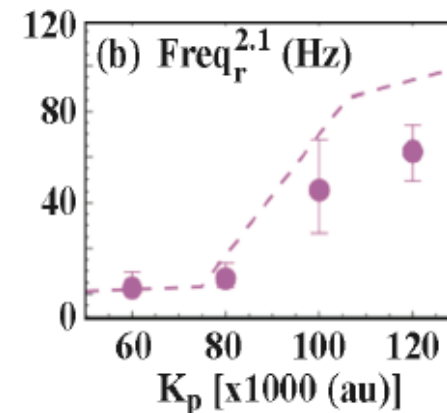
Avoidance of tearing mode locking and disruption with electro-magnetic torque introduced by feedback-based mode rotation control in **DIII-D** and **RFX-mod**



DIII-D



RFX

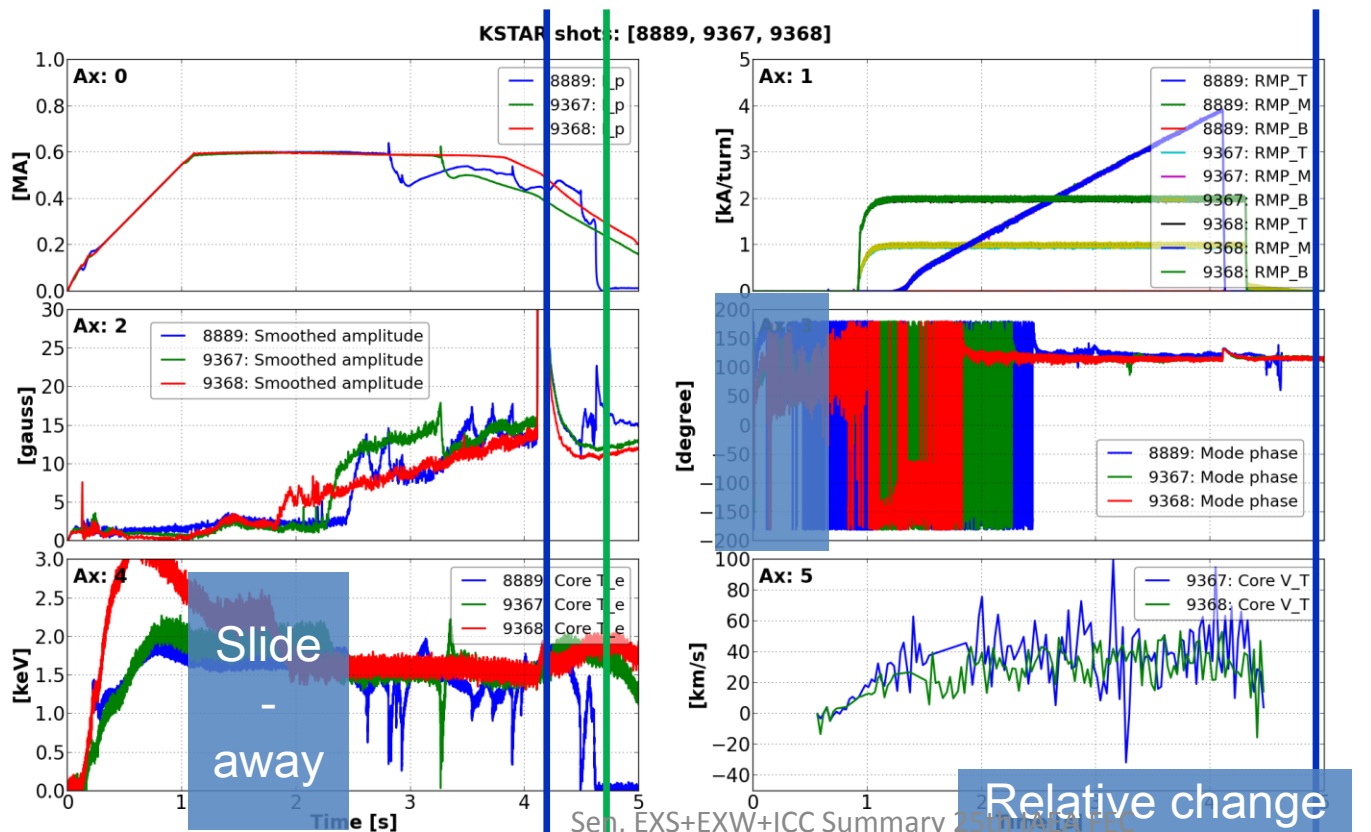


Plasma is less susceptible to minor disruption of n=1 locked mode under stronger n=2 even field.

Early disruption

#8889 (no n=2) > #9367 (n=2, 1 kA/t) > #9368 (n=2, 2 kA/t)

No disruption

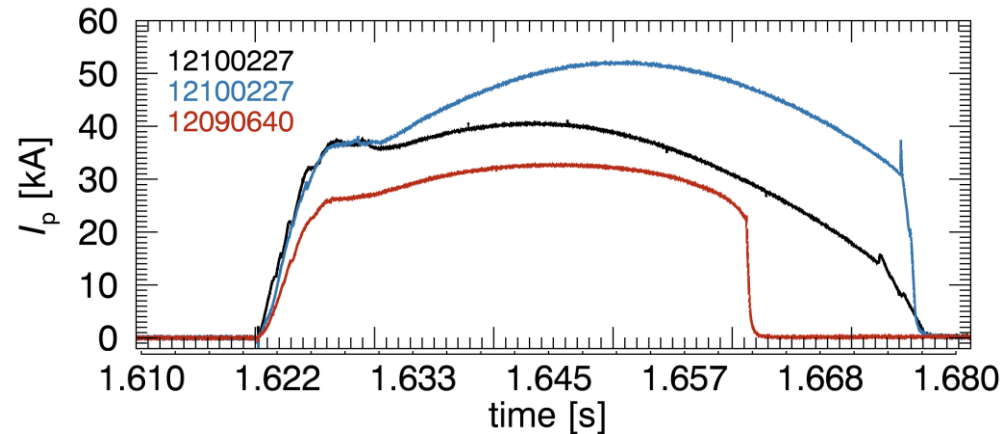


KSTAR

Disruption Avoidance / Control

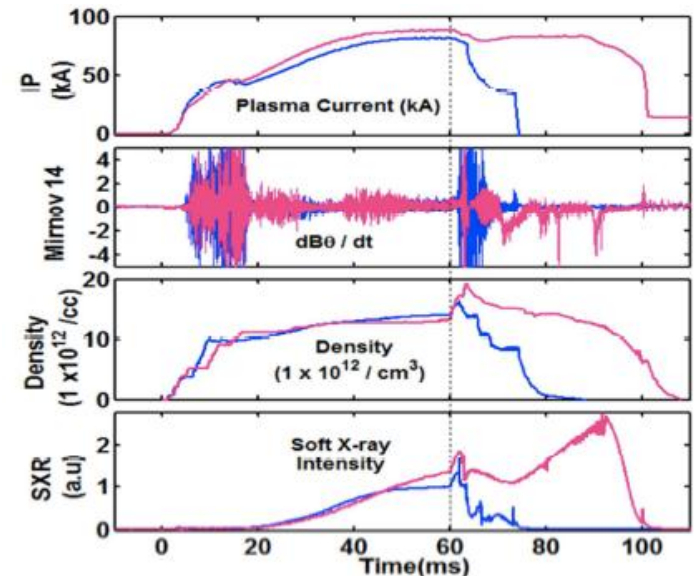
EX/P4-18, Maurer

Strong 3D equilibrium shaping, applied to tokamak like discharges on the **Compact Toroidal Hybrid (CTH)** expand its disruption free operating regime



EX/5-3, Tanna; EX/P7-16, Kulkarni; EX/P7-17, Dhyani

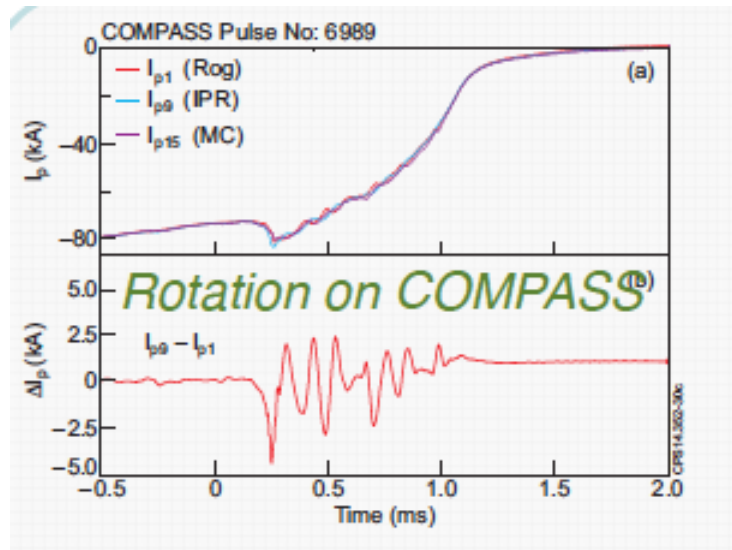
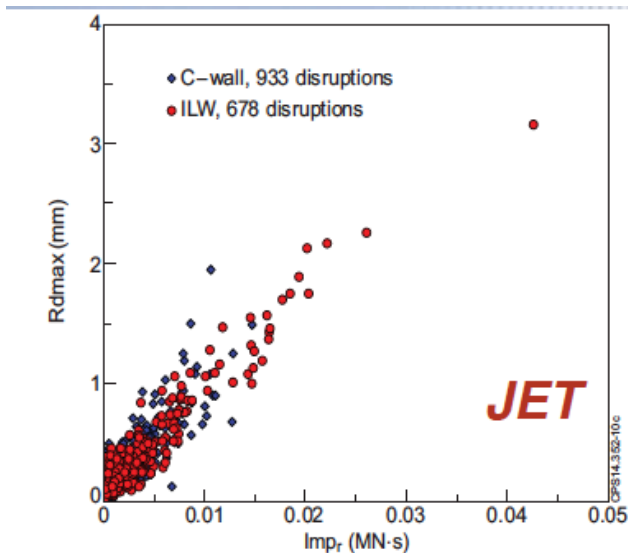
- Disruption control using biased electrodes in ADITYA tokamak to control MHD modes
- Similar effects also observed with the use of ICRF at the edge



Asymmetrical Disruptions in JET and COMPASS

P5-33, Gerasimov

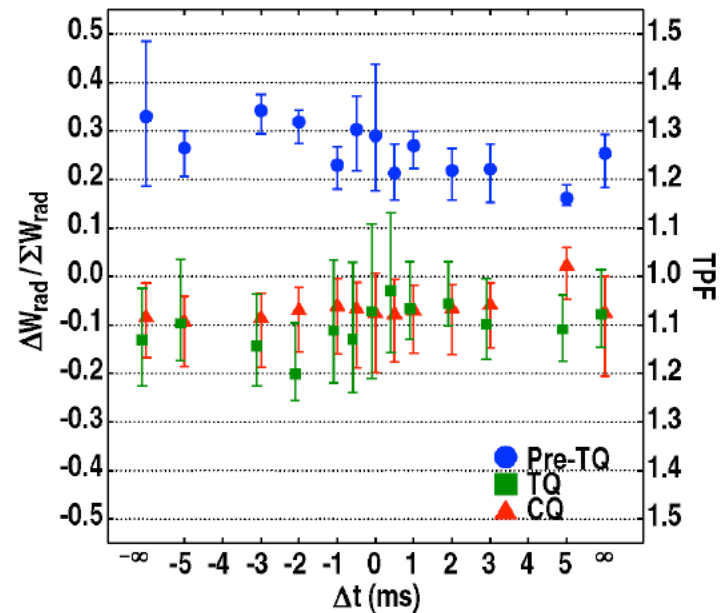
- Highlights the frequent occurrence of asymmetric disruptions in JET and the magnitude of their consequent sideways forces
- Resonance rotation with the natural vessel frequencies
- 3D JET model calculations for vessel poloidal currents
- Comparison with COMPASS data – consistency in terms of amplitude of asymmetry and rotation behaviour



Thermal and Current Quench Mitigation

EX/P2-22, Eidietis

- Measurement of Radiated Power Asymmetry During Disruption Mitigation on the DIII-D Tokamak
- radiation asymmetry during the thermal quench (TQ) and current quench (CQ) is largely insensitive to the number or location of injection sites
- application of an n=1 error field can modify the magnitude of the asymmetry during the TQ, supporting recent modeling results that indicate n=1 MHD during the TQ may be a cause of the radiation Asymmetry
- **results provide a firmer understanding of the 3D physics affecting the ITER DMS design**



- Massive gas injection radiation **efficiency decreases down to 75%** at high plasma thermal energy content ($W_{th}/(W_{th}+W_{mag}) = 0.5$)
- Toroidal radiation asymmetries depend on mode lock phasing before the disruption.
- Runaway electrons at JET-ILW can be produced in similar conditions as with the carbon wall using argon MGI
- **Runaway electron beams can be stopped if low-Z gas (D_2) is injected before the thermal quench**
- Mitigation of **already accelerated beams** (during current quench) using either high-Z or low-Z gases is **ineffective** in the mitigation pressure range tested.
- Impacts of ~ 770 kA RE beam leads to significant melting of PFC.
- **Radiation asymmetries studies** using two disruption mitigation valves are planned.
- **Investigation of mitigation of an already accelerated runaway** beam using higher pressures is planned
- Investigation of **runaway beams relation to vertical stability, control and plasma shape** is to be continued

- Massive gas injection radiation **efficiency decreases down to 75%** at high plasma thermal energy content ($W_{th}/(W_{th}+W_{mag}) = 0.5$)
- Toroidal radiation asymmetries depend on mode lock phasing before the disruption.
- Runaway electrons at JET-ILW can be produced in similar conditions as with the carbon wall using argon MGI
- Runaway electron beams stopped **only** by low-Z gas injected before current quench
- Mitigation of already accelerated beams (during current quench) using either high-Z or low-Z gases is **ineffective** in the mitigation pressure range tested.
- Impacts of ~770 kA RE beam leads to significant melting of PFC.
- **Radiation asymmetries studies** using two disruption mitigation valves are planned.
- **Investigation of mitigation of an already accelerated runaway** beam using higher pressures is planned
- Investigation of **runaway beams relation to vertical stability, control and plasma shape** is to be continued

Runaway Generation / Control

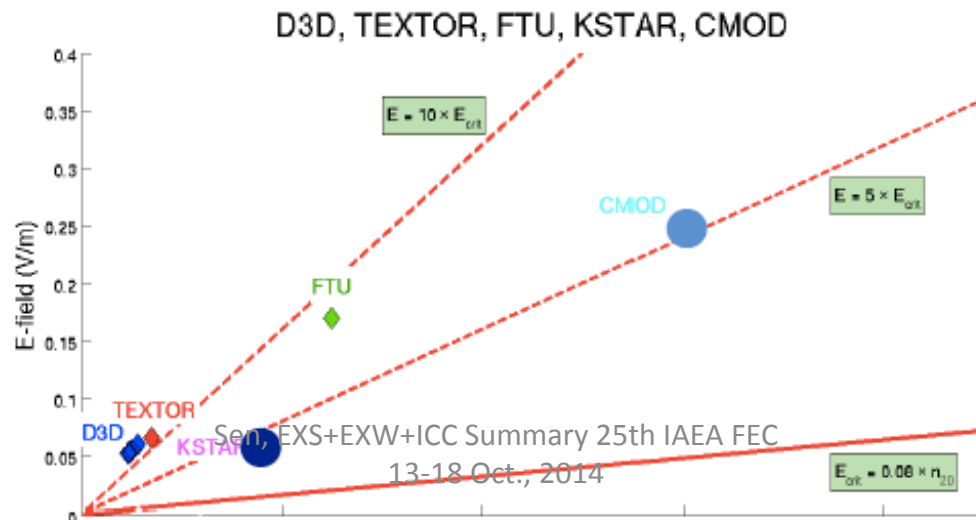
An ITPA joint experiment to study runaway electron generation and suppression

A study of runaway electrons under well-controlled, well-diagnosed conditions in a number of tokamaks finds that the threshold E -field for both onset and decay of runaway electron (RE) signals is at least 4 – 5 times above the Connor-Hastie E_{crit}

- Conversely, the density at which RE's are suppressed for a given loop voltage is at least a factor of 4-5 less than theoretically predicted

This suggests that there are other significant RE loss mechanisms in addition to collisional damping, even in steady-state quiescent plasmas.

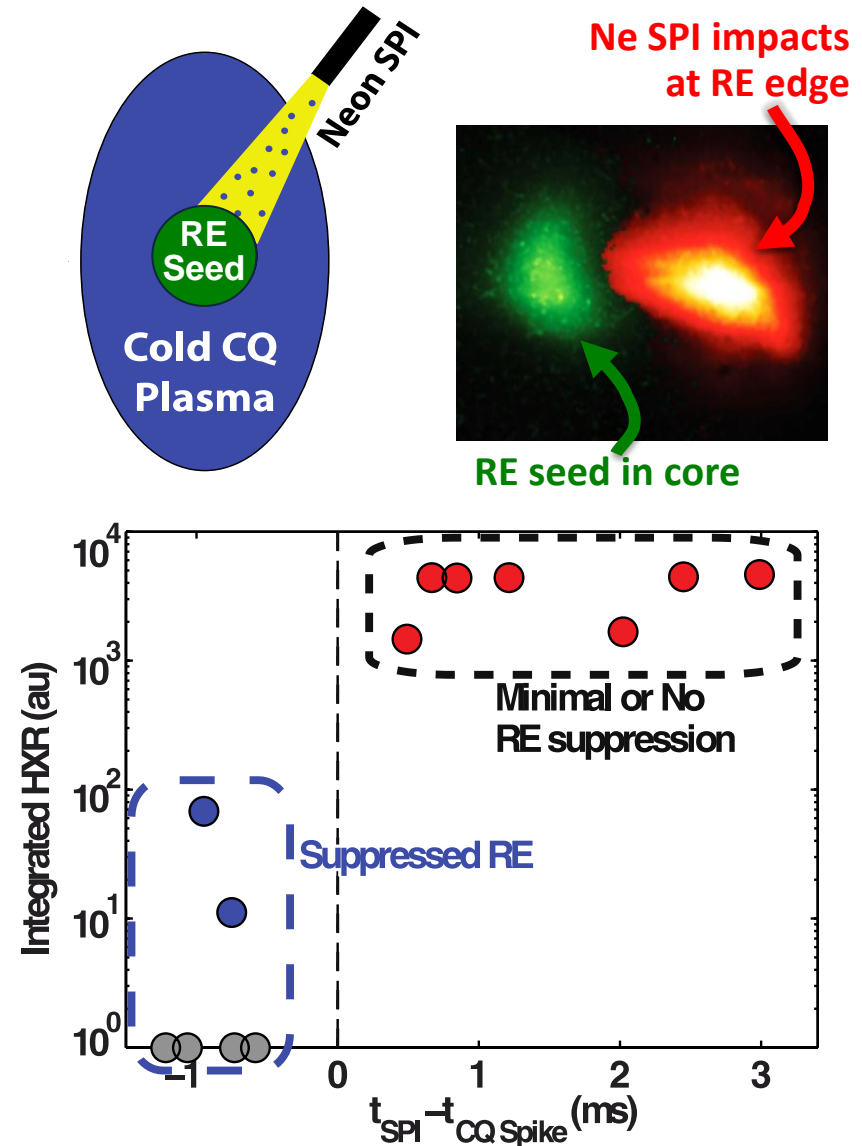
It also suggests that mitigating runaways on ITER may not require fueling to the Rosenbluth density.



DIII-D Expt on RE Mitigation using SPI

- Injection of Ne Shattered Pellets into **early** CQ is effective in suppressing runaway growth
- RE current dissipation explained by RE-ion pitch angle scattering
 - Higher Z more effective at RE dissipation

EX/PD/1-1, Eidietis



ELMS – Characterization / Mitigation / Suppression

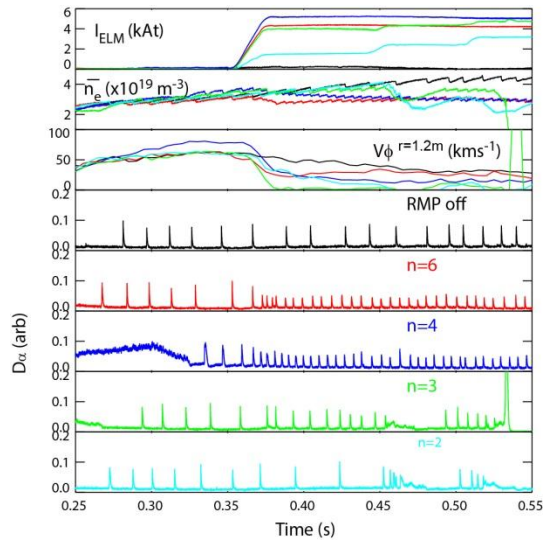
Progress since 2012 FEC

- **RMP ELM mitigation and suppression of Type I ELMs**
 - ✓ **Expanded operating space**
 - ✓ **Shown to be robust to loss of coils (reassuring for ITER)**
- **Alternate external suppression methods appear promising**
 - **Pellet pacing, SMBI, gas injection, LHW,...**
- **Improved understanding of ELM dynamics from better diagnostic measurements and modeling studies – also some challenges**

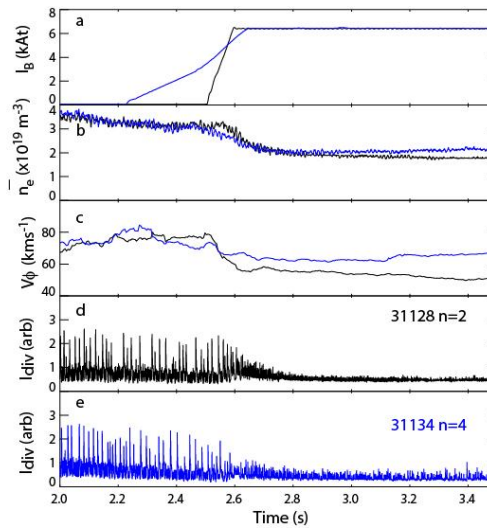
Expanded Operating Space

EX/1-2, Kirk

MAST



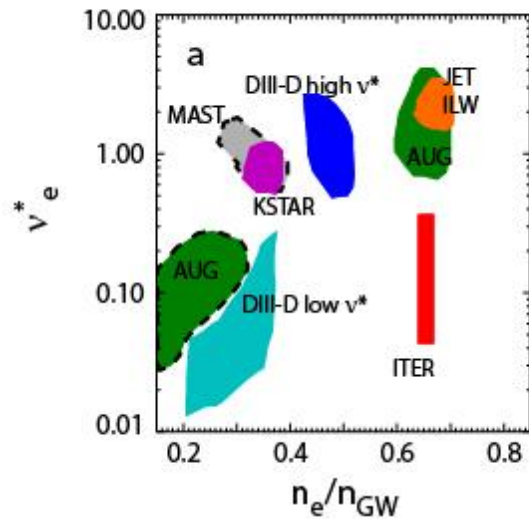
AUG



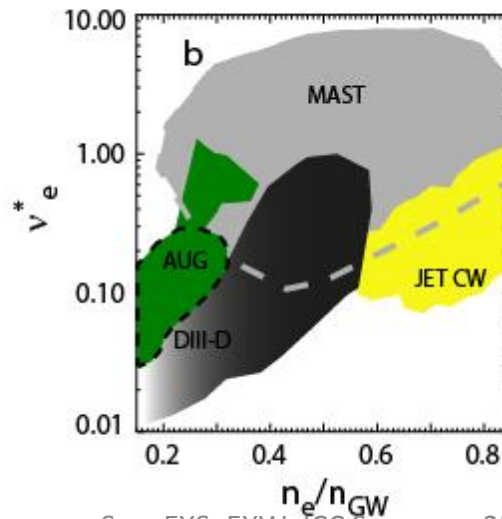
Sustained ELM mitigation/type I ELM suppression has been achieved on MAST and AUG with magnetic perturbations with a range of toroidal mode numbers

ELM size and target heat loads are reduced but at a price of a reduction in confinement

type I ELM suppression



type I ELM mitigation

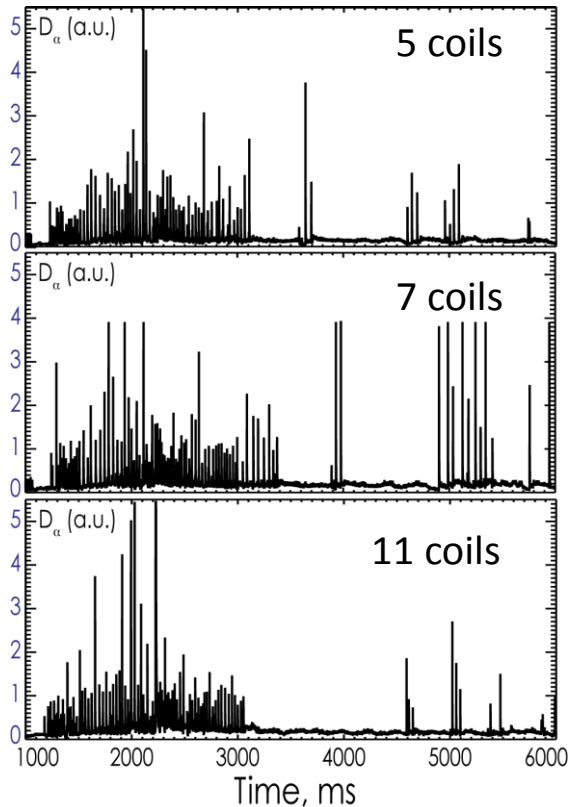


Dashed curves expanded operating space for the type I ELM suppression/mitigation from MAST and ASDEX Upgrade

Results show that regimes with tolerable ELMs can be established over a wide operating space in a range of devices

Advances in Basic Understanding of ELM Suppression

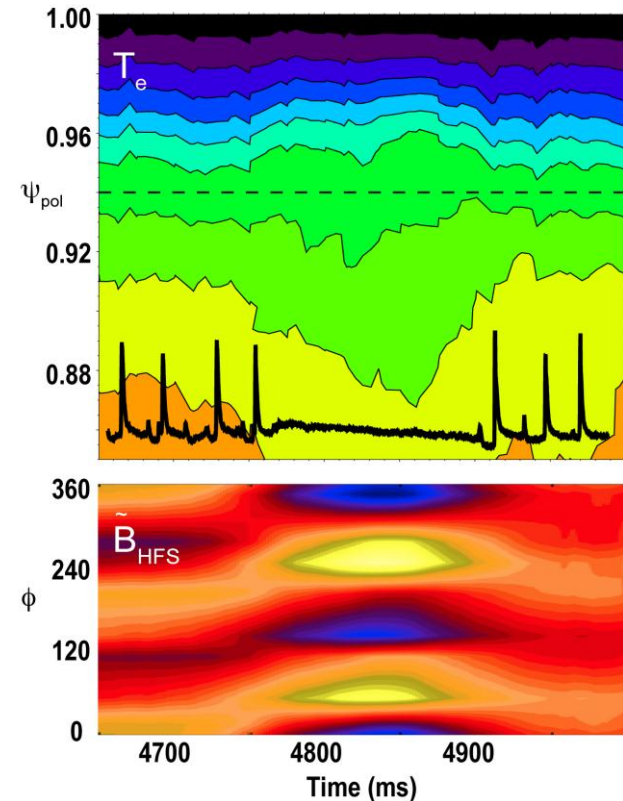
- ELM suppression achieved with as few as 5 internal coils



DIII-D results

EX/1-1, Wade; EX/P2-21, Orlov

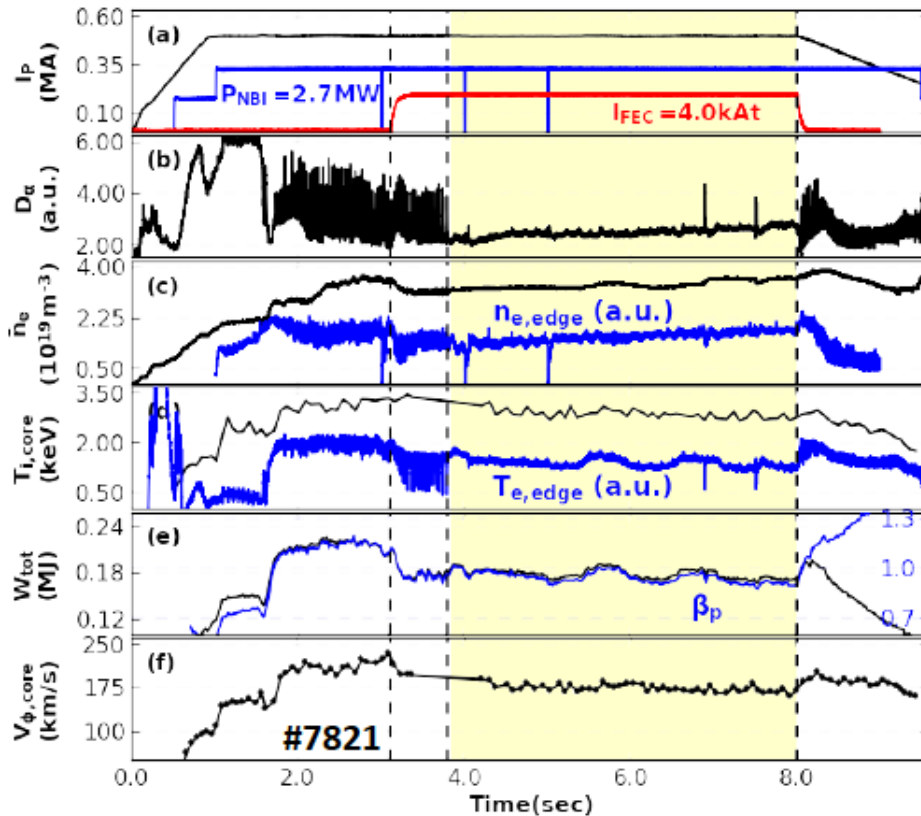
- New data reveals bifurcation indicative of resonant field penetration at ELM suppression



Highlights importance of plasma response to RMP fields

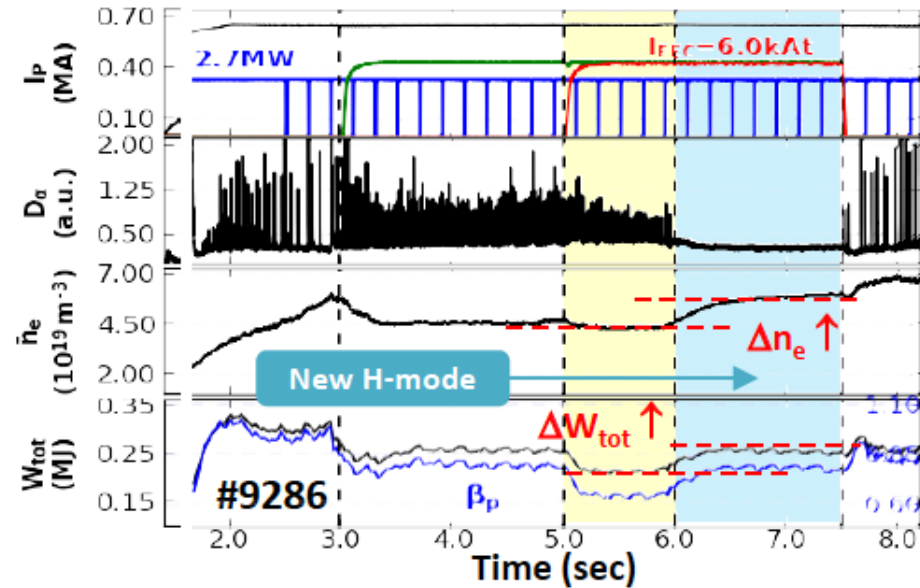
Successful ELM-Suppression Using Low n RMPs and Its Understanding as a New ('bursty') H-Mode State

EX/1-5, Jeon



- Long ELM suppression (> 4.0 sec)
- ELM-suppressions by low n RMPs
- Wide range of q_{95}
 - n=1 RMP for $q_{95}=5.5\sim 6.0$ (high)
 - n=2 RMP for $q_{95}=3.7\sim 4.0$ (low)

KSTAR

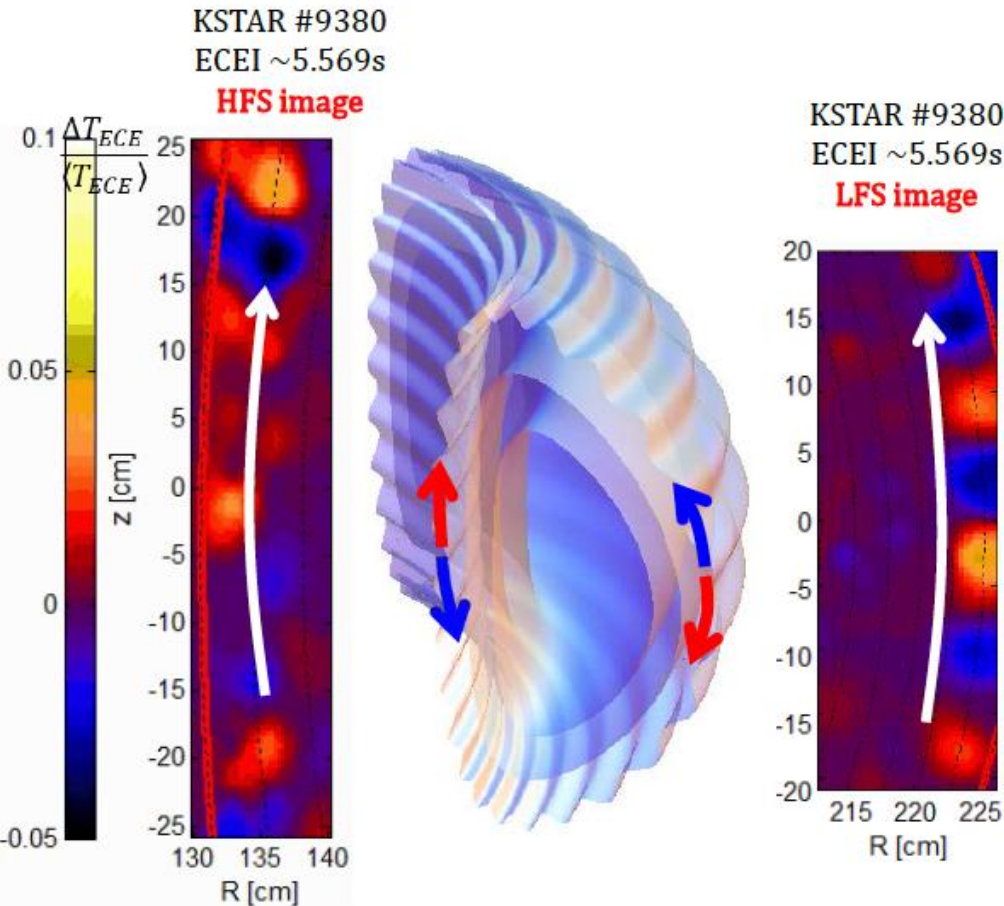


- Two stationary ELM states under same RMP field
 - Mitigated ELMs : confinement ↓
 - Suppressed ELMs: confinement ↑
- A possibility of ELM suppression without confinement reduction
- ELM-suppression = a new state of H-mode (so called, 'bursty' H-mode)

2014-10-14

IAEA-FEC-2014-YMJ

Simultaneous Measurement of ELMs at both High and Low Field Sides in KSTAR

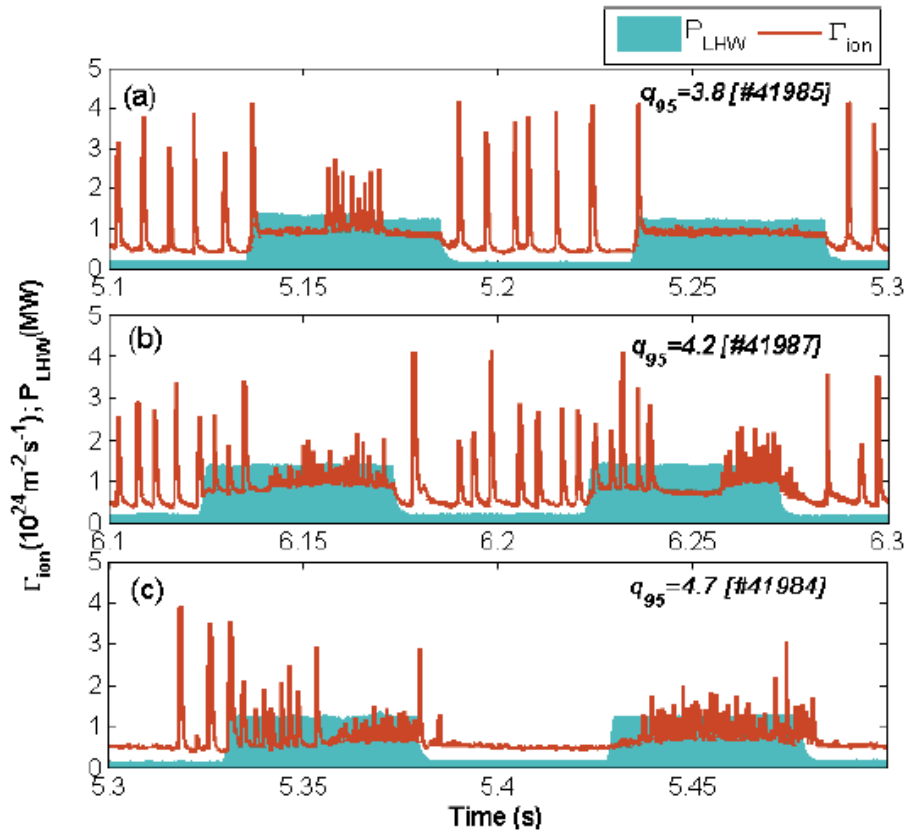


- Comparable mode strength at HFS and LFS
- Asymmetries in toroidal/poloidal rotation velocities
- Mode structure at HFS not consistent with Ballooning Mode model
- Mode numbers different on the two sides

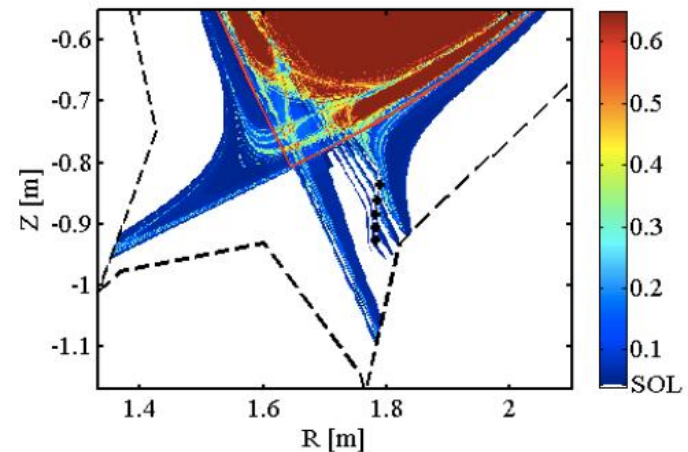
EX/8-1, Park

ELM mitigation by Lower Hybrid Waves in EAST

EX/P3-8, Liang



- ELM mitigation with LHW obtained over a wide range of q_{95}
- Attributed to formation of helical current filaments in SOL
- ELM freq. increases from 150 Hz to about 1 KHz



Strong modification of plasma edge

Other MHD and 3D physics studies

- Improved understanding of Neoclassical Toroidal Viscosity (NTV) in tokamaks
- Feedback control of RWM allows tokamak operation at $q_{95} \leq 2$
- Helical modes observed in KSTAR
- Basic studies of MHD instabilities

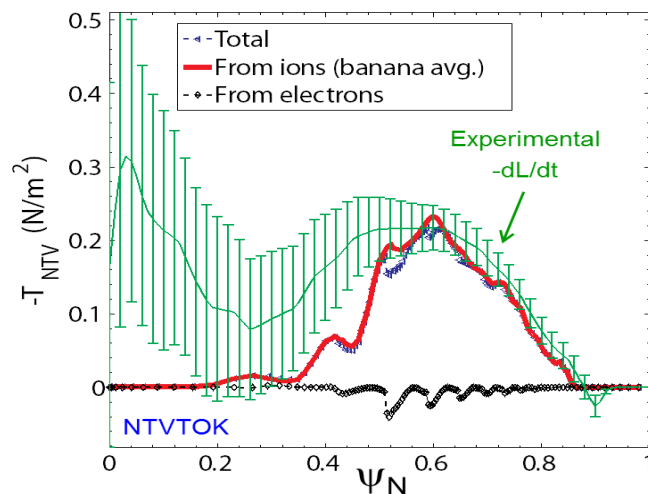
Neoclassical Toroidal Viscosity for Rotation Control and the Evaluation of Plasma Response

EX/1-4, Sabbagh

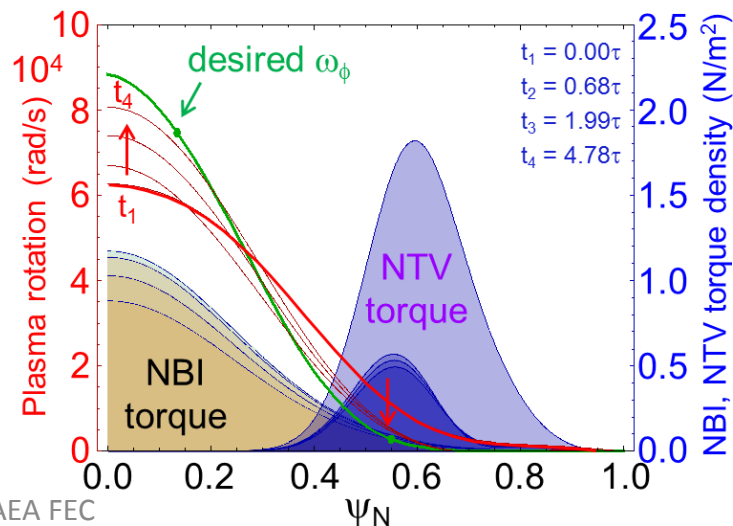
Highlights

- **Experimental NTV characteristics**
 - NTV experiments on NSTX and KSTAR
 - NTV torque T_{NTV} from applied 3D field is a radially extended, relatively smooth profile
 - Perturbation experiments measure T_{NTV} profile
- **Aspects of NTV for rotation control**
 - Varies as δB^2 ; $T_{NTV} \propto T_i^{5/2}$ in primary collisionality regime for large tokamaks
 - **No hysteresis** on the rotation profile when altered by non-resonant NTV is key for control
 - Rotation controller using NTV and NBI tested for NSTX-U; model-based design saves power
- **NTV analysis to assess plasma response**
 - Non-resonant NTV quantitatively consistent with fully-penetrated field assumption
 - Surface-averaged 3D field profile from M3D-C¹ single fluid model consistent with field used for quantitative NTV agreement in experiment

Perturbation experiments measure NTV torque profile and compare to theory

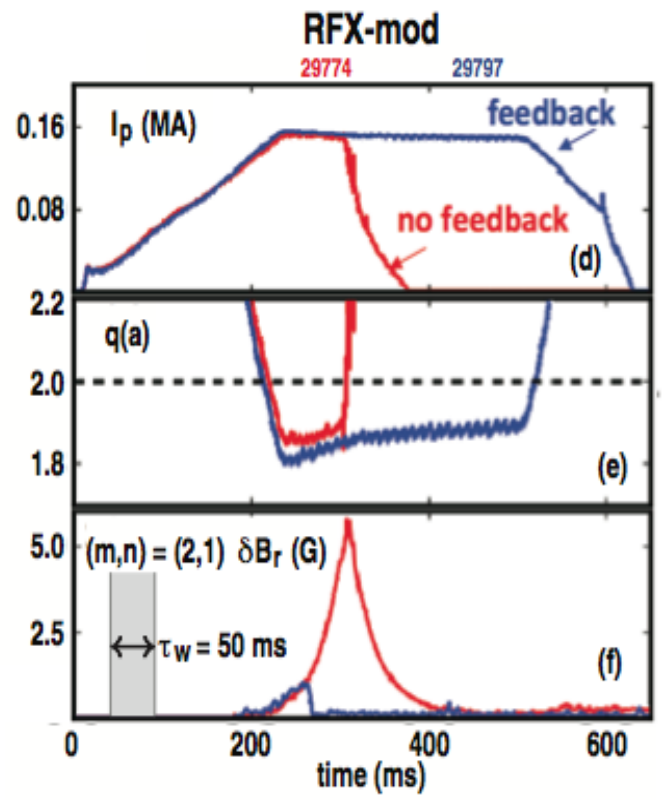
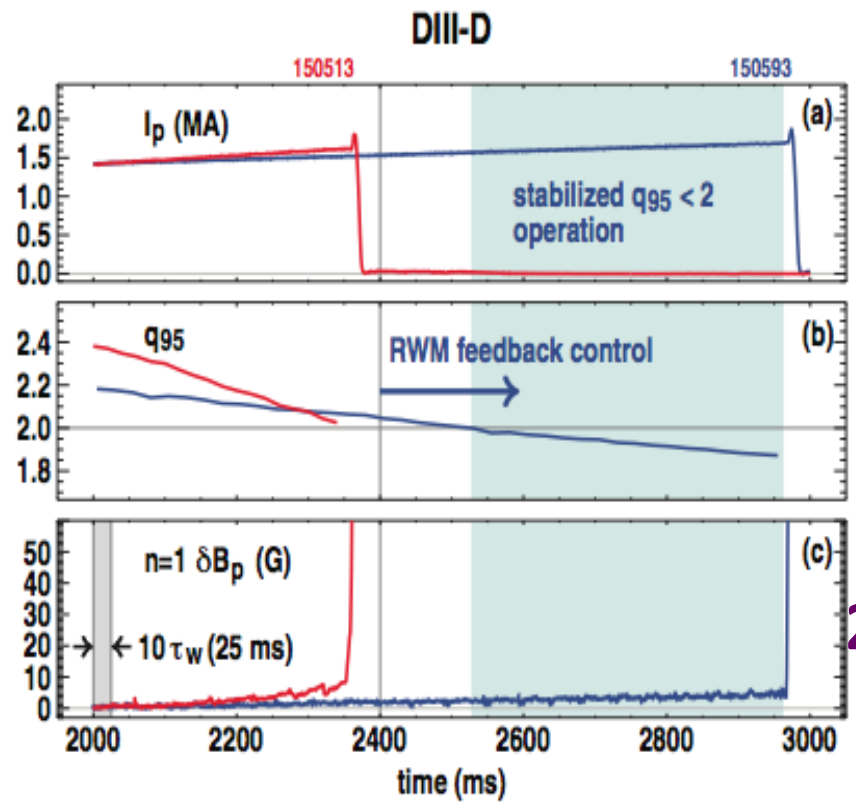


Rotation controller using NTV and NBI



DIII-D and RFX-mod achieved reproducible tokamak operation at $q_{95} < 2$ thanks to feedback control of 2/1 RWM – for many resistive wall times using 3D magnetic fields

EX/P2-41, Martin



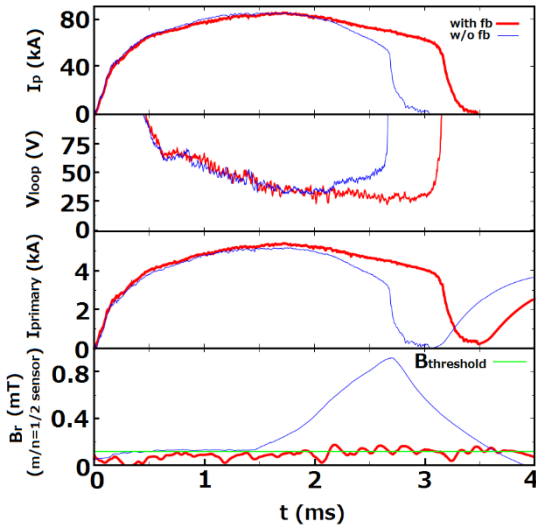
I_p

q_{95}

2/1 RWM

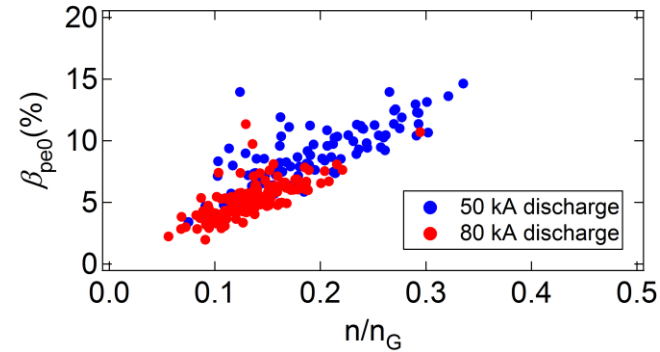
Blue curve: with feedback control
Red curve: w/o feedback control

Active MHD control has resulted in RWM-stabilized, high- β_p , low-A RFP plasmas, and two routes to helical RFP states are identified



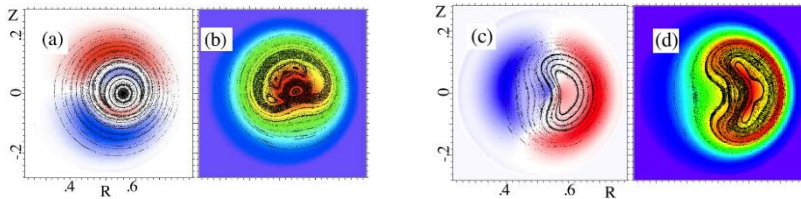
Using saddle coil array for feedback MHD control, **RWM was suppressed** and the RFP discharge duration could be extended to the upper bound determined by the iron core saturation.

Definition: $\beta_p = 2\mu_0 p_{e0} / B_{pa}^2$

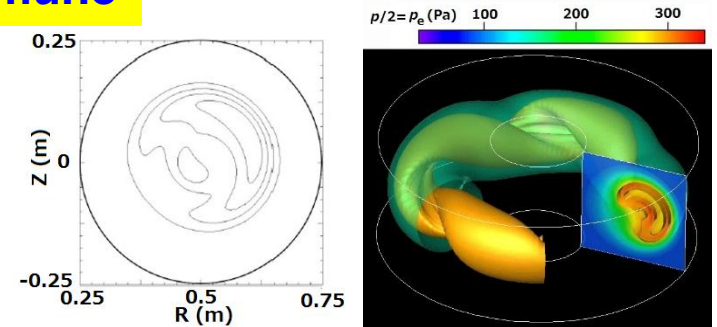


Central electron pressure vs. I_p^2 shows that feedback stabilization of RWM has led to improved performance with attainment of **electron poloidal beta 10~15%**. Density limit studies are becoming important in low-A RFP.

EX/P3-52, Masamune



Growth of **both the resonant (left) and non-resonant (left) mode can lead to self-organized helical RFP** with almost identical deformation. Resonant mode accompanies reconnection (MIPS simulation).



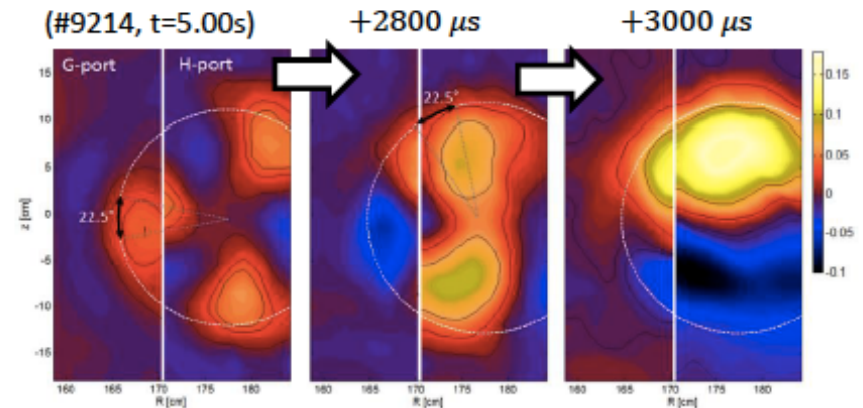
Reconstructed magnetic surface shape using SXR CT during QSH phase shows good agreement with helical equi-pressure surface shape in 3-D MHD simulation using the MIPS code.

EX/P8-12: Helical modes induced by localized current perturbations in sawtoothing KSTAR plasmas

G.S. Yun
POSTECH, Korea

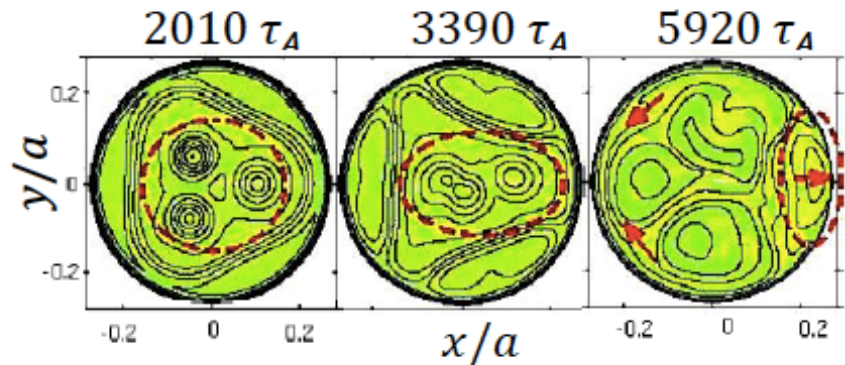
Multiple flux tubes (MFTs), a universal feature in plasmas with localized ECH heating

- Dynamics of MFTs visualized by 2D imaging: **growth, steady-state (\sim ms), merging ($\sim 10 \mu$ s), and crash ($\sim 10 \mu$ s).**
- Number of flux tubes strongly depends on the **ECH position relative to $q=1$ surface.**



Nonlinear Reduced MHD simulation with an empirical current source model:

- 1) **Flat q -profile** ($|1 - q| < 0.5\%$) after crash
- 2) Growth and saturation of **$m/n=1/1$ helical flux tubes driven by localized ECH**
- 3) **Merging of flux tubes**



Ongoing study focuses on:

- 1) Dependence on the ECH injection angle (i.e., width and amount of the driven current)
- 2) Identification of q profile after sawtooth crash
- 3) Self-consistent modeling of the ECH coupling with the flux tubes

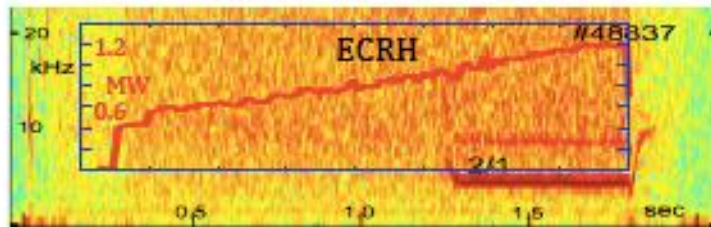
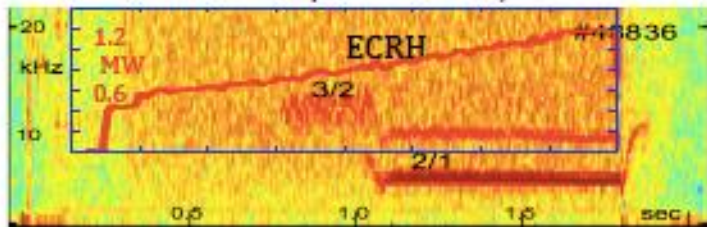
(R)MHD INSTABILITIES – BASIC STUDIES

Questions addressed: Triggering mechanisms, Mode Dynamics

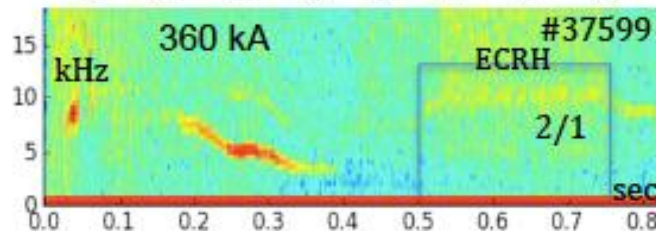
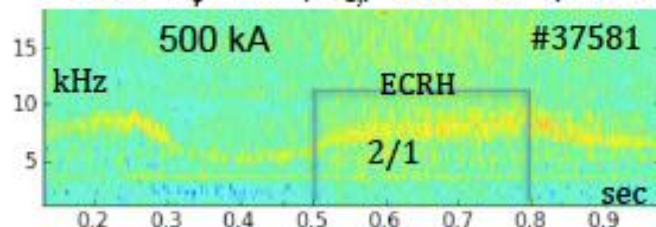
FTU & TCV:

- 2/1 TM triggered by Ne injection **EX/P2-53, Botrugno**
- TM onset by central EC power deposition **EX/P2-54, Nowak**

TCV: -115 kA , $B_\phi = -1.4 \text{ T}$, $n_{e,l} = 1.6 \cdot 10^{19} \text{ m}^{-3}$



FTU: $B_\phi = 5.3 \text{ T}$, $n_{e,l} = 4 \cdot 10^{19} \text{ m}^{-3}$ (#37599) - $6 \cdot 10^{19} \text{ m}^{-3}$ (#37581)

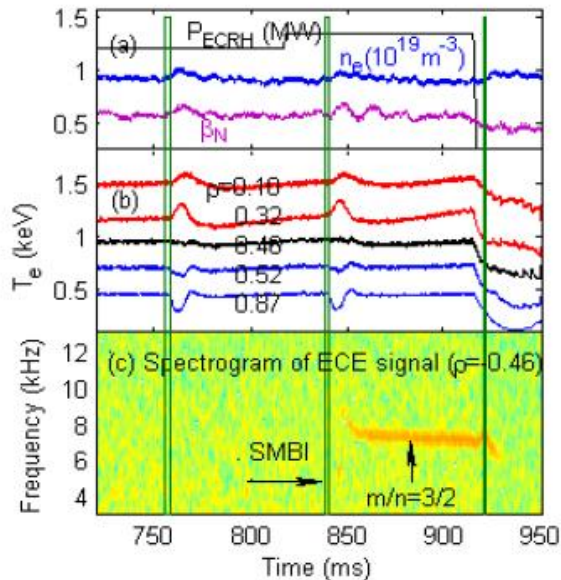


2/1 in counter- I_p direction

freq. increase due to the co-ECCD torque

HL-2A:

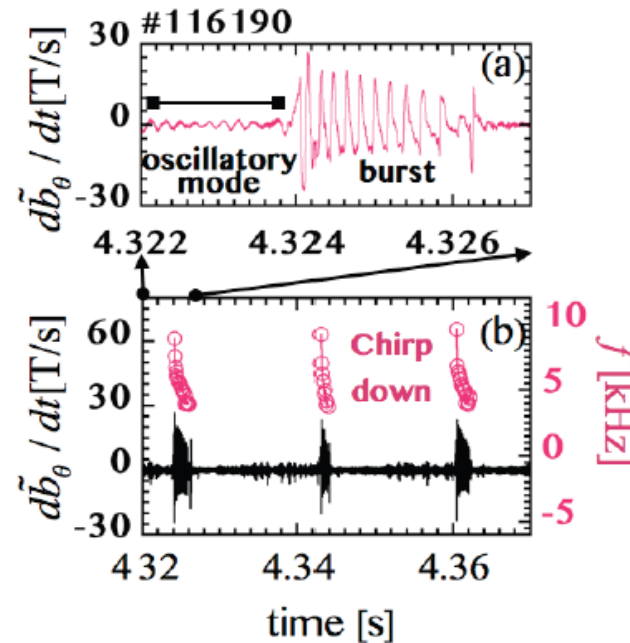
- NTM triggered by intrinsic error fields **EX/P7-19, Xu**
- **NTM triggered by non-local transport EX/6-4, Ji**
- Interaction between MHD modes **EX/P7-25, Yu**



SMBI induced NLT

LHD:

- Effects of low n MHD modes on achievable beta values **EX/P6-37**
- **Bursting Resistive Interchange Modes EX/P6-36**



Energetic-Ion-Driven-Resistive Interchange Mode (EIC)

Energetic Particles / Waves

Main Issues

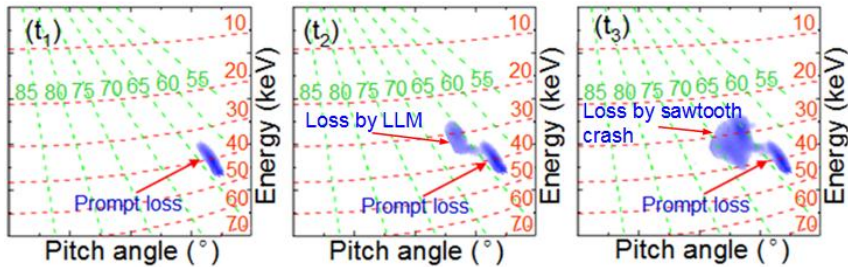
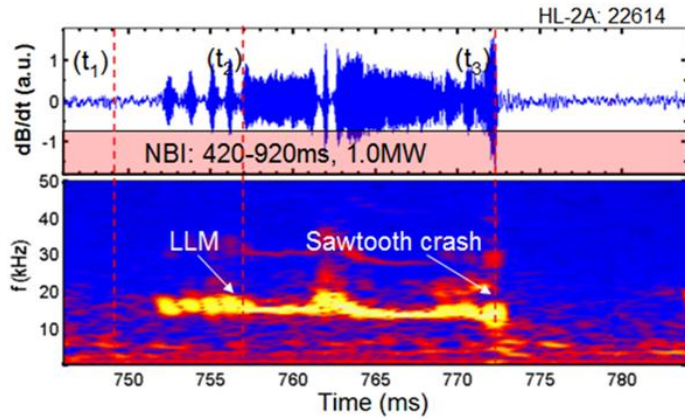
- Good confinement of EPs crucial for α heating of burning plasmas
- Instabilities driven by EPs can degrade their confinement and also alter their energy distribution; also impact on NB-CD
- Characterization of stability boundaries
- Better understanding of fast ion transport

Progress since 2012 FEC

- Improved diagnostics, better nonlinear modeling have furthered our understanding on a number of issues
- Exptal database extended to include STs, stellarators, RFPs etc.
- Provide more accurate correlations between fast ion losses & instabs.

HL-2A

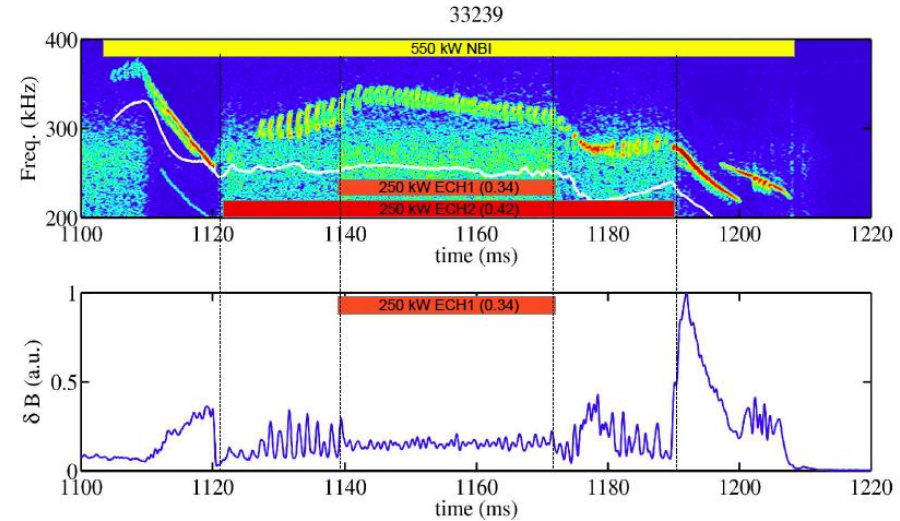
EX/P7-24, Zhang



Utilizing a new scintillator-based lost fast-ion probe, recent HL-2A experiments have elucidated a variety of neutral beam ion loss behaviors in the presence of MHD instabilities.

TJ-II

EX/P4-46, Cappa

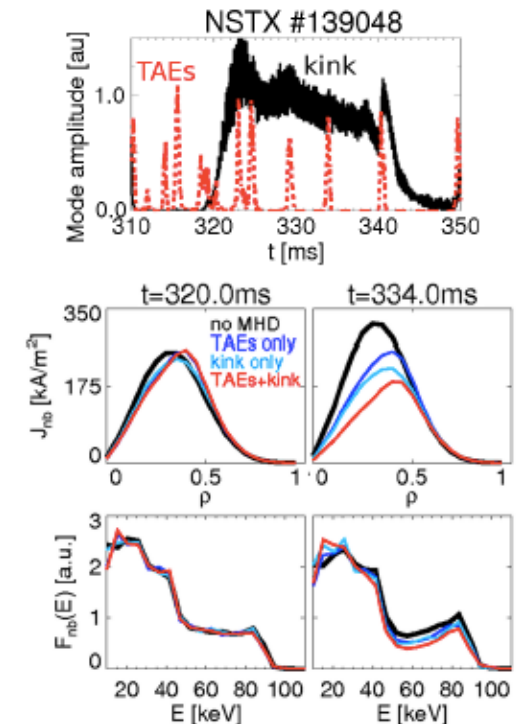
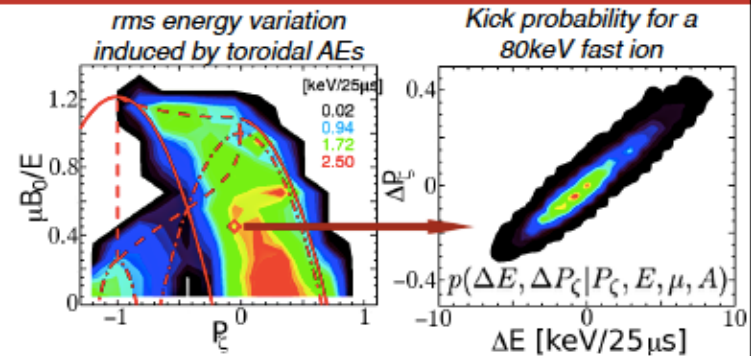


ECRH has a strong influence on the NBI driven Alfvén modes in TJ-II. A second EC beam can stabilize the AE.

EX/10-4: Effects of MHD instabilities on Neutral Beam current drive

M. Podestà, M. Gorelenkova, D. S. Darrow, E. D. Fredrickson, S. P. Gerhardt, W. W. Heidbrink, R. B. White

- Neutral Beam heating and current drive are crucial for the success of ITER, Fusion Nuclear Science Facility (FNSF)
- MHD instabilities (e.g. Alfvénic modes, AEs) can reduce NB-CD efficiency
- A new model is developed to quantify and predict AE effects on NB-CD [Podestà, PPCF 56 (2014) 055003]
 - Fast ion evolution is consistently treated *in phase space* (energy, canonical angular momentum, magnetic moment)
 - Interactions modeled through *kick probability* $p(\Delta E, \Delta P_\zeta | E, P_\zeta, \mu)$
 - Implementation in the transport code TRANSP under way
- Results from NSTX confirm strong effect of AEs on NB-CD
 - Up to 40% of local current density can be redistributed
 - Effects not correctly accounted for by models based on *ad-hoc* spatial diffusion



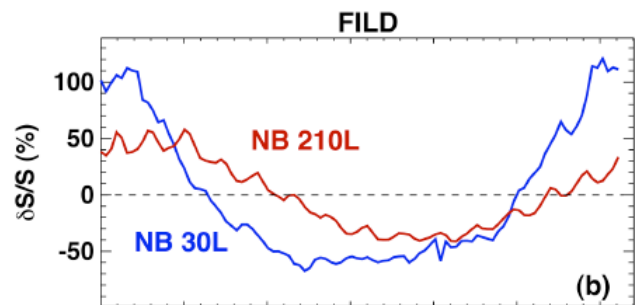
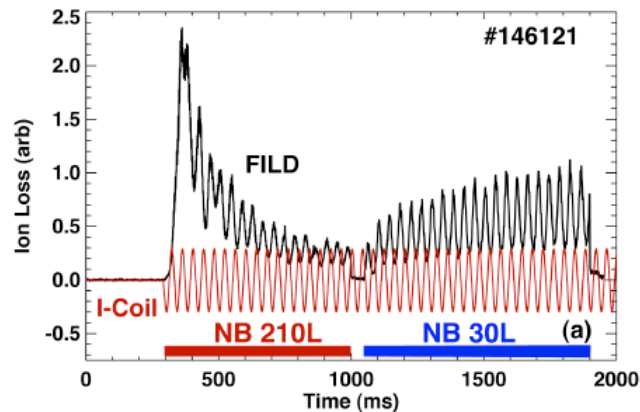
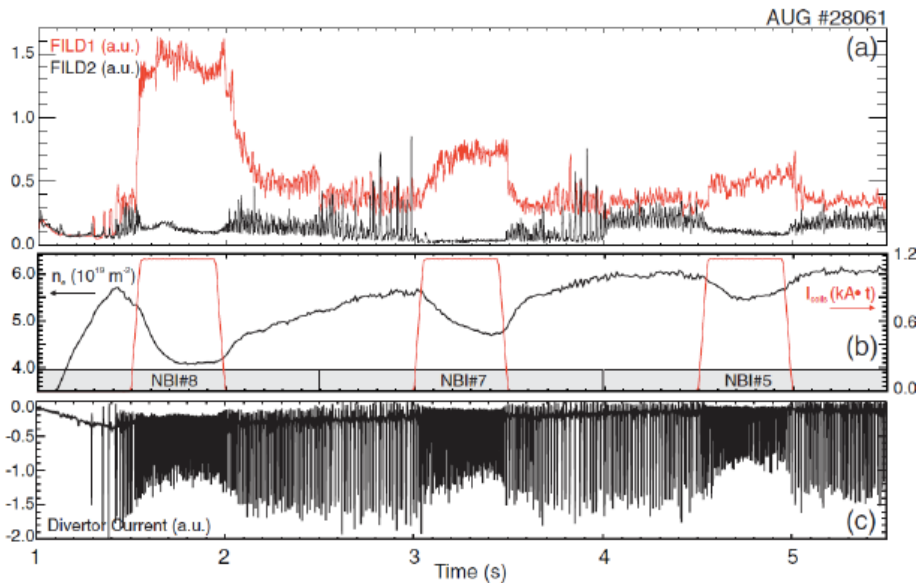
Fast-ion response to externally applied 3D magnetic perturbations

ASDEX-U

EX/P1-22, Garcia

DIII-D

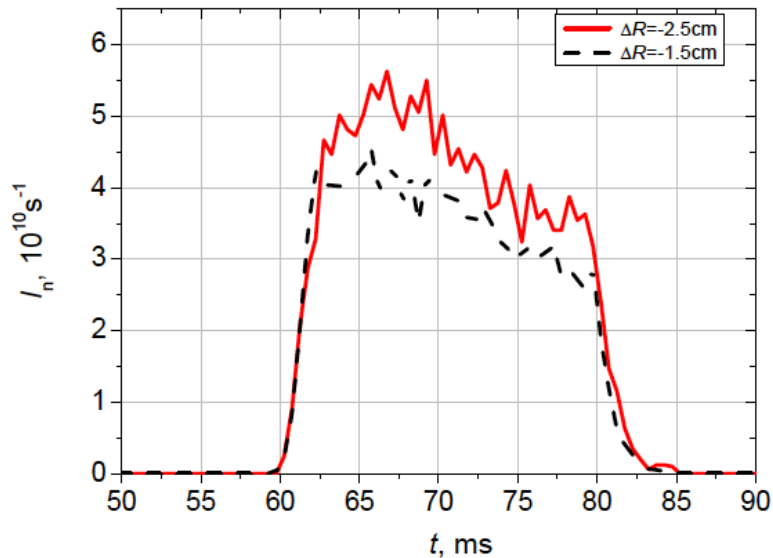
EX/10-2, Van Zeeland



strong plasma & fast-ions response is observed in H-mode regimes with low collisionality / density and low q_{95} .

Pitch angle and energy resolved measurements + wide field-of-view infrared imaging show fast ion losses correlated with applied 3D fields. in L-mode plasmas. Good agreement with model simulations.

TUMAN -3M



Plot of neutron flux vs time for different inward shifts of column

GLOBUS-M

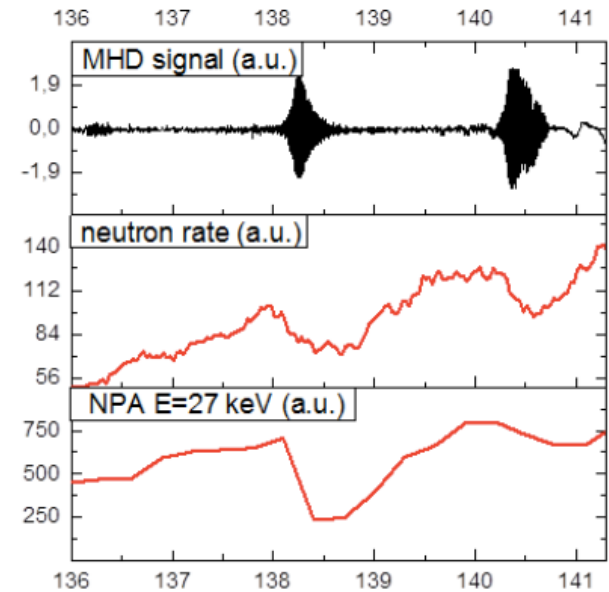


Fig.2 – Losses during TAE in $D \rightarrow D$ experiments

- Particle losses highly correlated with TAE
- Sawteeth induced losses >25%
- Shift in plasma column inwards can reduce losses

Noninductive Current Drive

- Studies of LHCD physics and applications
- ICRH optimization in JET
- Solenoid-free ST startup

Near-Field Physics of Lower-Hybrid Wave Coupling

EX/4-2, Goniche

Tore Supra

Large data base (~230 points) indicate that E_{RF} scales as $(P_{coupled})^{1/2}$ assuming edge density near the cut-off density ($\sim 2 \times 10^{17} m^{-3}$)

EX/P6-17, Parker

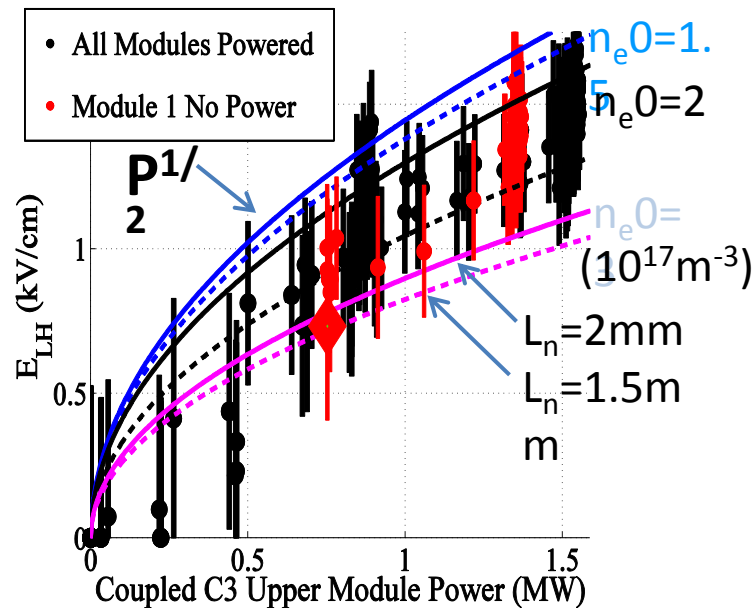
Alcator C-MOD

Loss of LHCD efficiency at high density is associated with Excitation of Parametric Decay Instabilities. PDI are excited near the separatrix and onset can be mitigated by modifying conditions in the scrape-off layer. **Launch from HFS may be more efficient – scheme for next machine.**

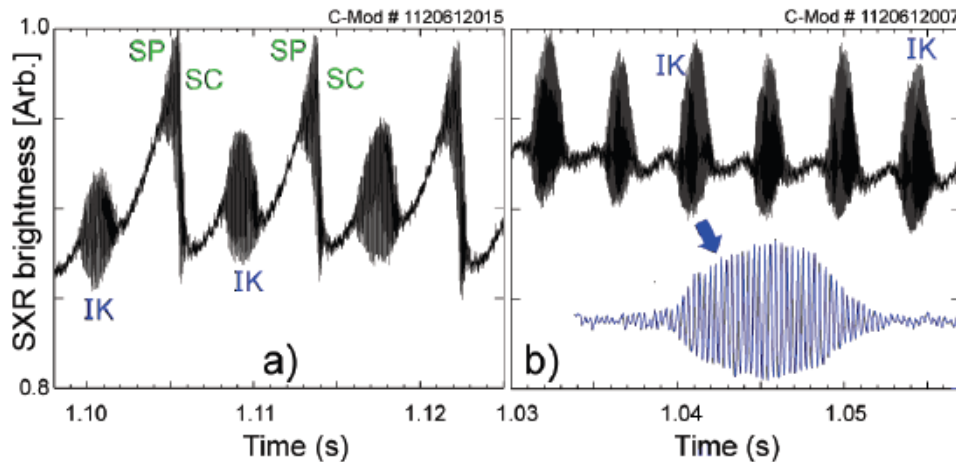
EX/P3-11, Ding

EAST

High density experiments with LHCD analyzed by simulation using experimental parameters, show that parametric instability, collision absorption in the edge region, and density fluctuations could be responsible for the low current drive efficiency at high density.



EX/P6-20, Delgado-Aparacio: Destabilization of Internal Kink by Suprathermal Electron Pressure Driven by Lower Hybrid Current Drive (LHCD)



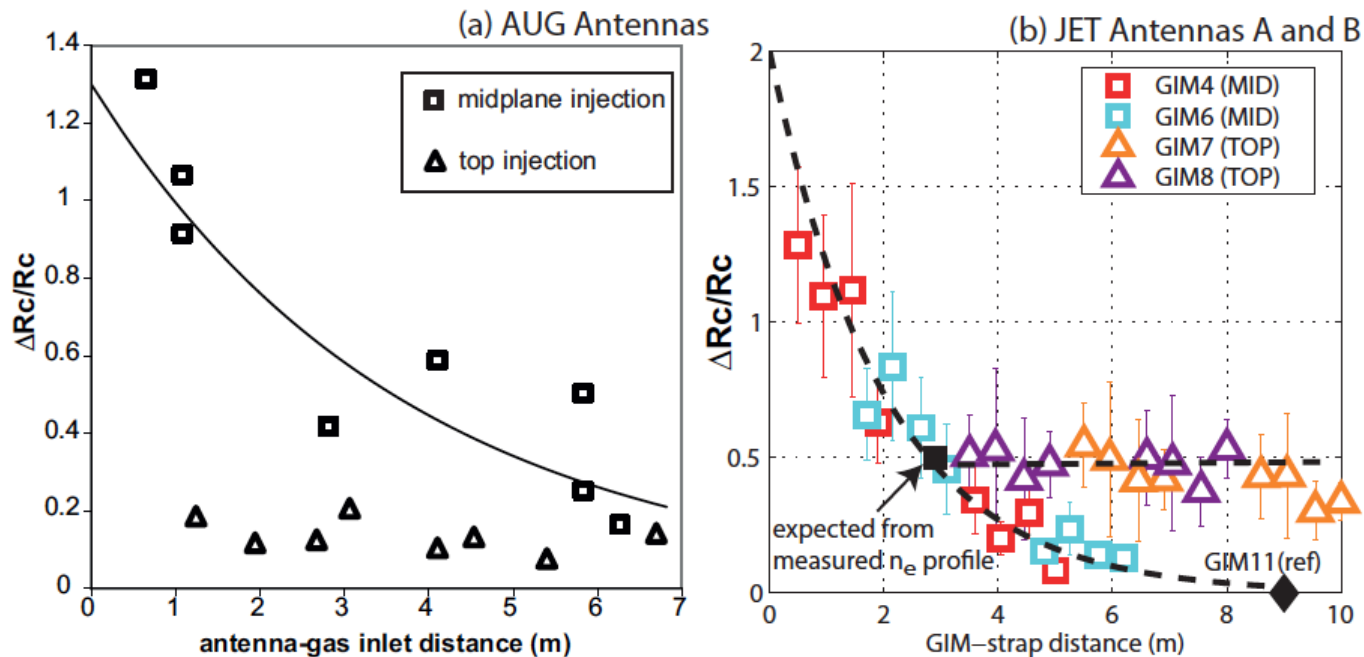
- *A new type of periodic fishbone-like instability with a (1,1) internal kink-like structure*
- *distinct from the sawtooth instability*

On-axis SXR signatures of a (1,1) internal kink-like (IK) mode in the a) presence or b) absence of Sawtooth precursors (SP) and crashes (SC).

Demonstrate a direct dynamic relation between LHCD generated fast electrons and a fishbone-like mode

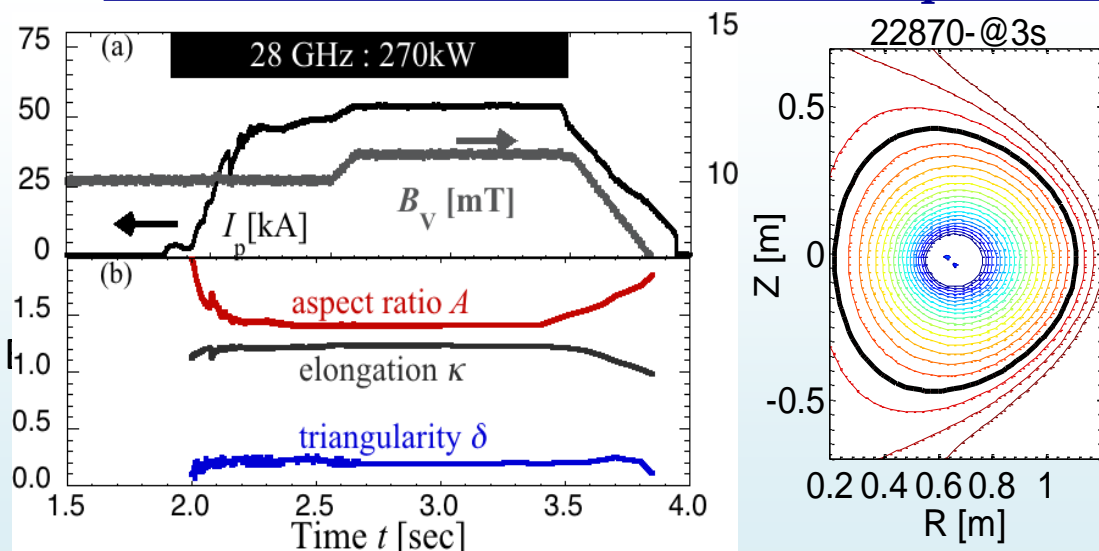


- Proximity between antenna and outer midplane (OMP) gas injection maximises the effect of local gas injection on ICRF antenna coupling resistance (JET, AUG, DIII-D).
- Top injection leads to a lower coupling improvement, toroidally uniform.
- To assess efficiency of local gas injection on ITER ICRF antenna coupling, need to take into account the field lines topology and use 3D SOL modelling codes.



Fully Non-inductive Current Drive Experiments using 28 GHz and 8.2 GHz Electron Cyclotron Waves in QUEST H. Idei, *et al.*

54 kA Plasma Sustainment in Low Aspect Ratio Config. by 28GHz Injection



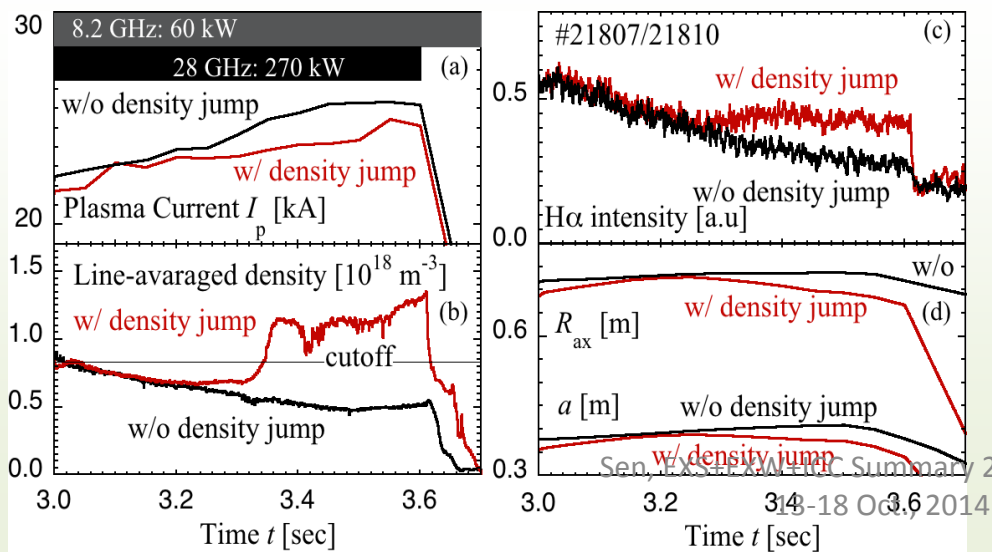
Plasma current of **54 kA** was non-inductively sustained for 0.9 sec by only 28 GHz injection.

Plasma shaping was almost kept for **1.3 sec.**

Higher current of **66 kA** was non-inductively obtained by slow ramp-up of vertical field also.

Non-inductive high current plasma start-up by 2nd ECH/ECCD has been demonstrated.

Over Dense Plasma Sustainment by 28 /8.2 GHz Injections after Spont Density Jump



Spontaneous density jump across the cutoff density was observed in superposed 28 and 8.2 GHz injections.

H α intensity was kept, magnetic axis R_{ax} and minor radius a were slightly decreased in the density jump case.

Plasma current I_p was once decreased, but was recovered after the plasma shaping became more stable.

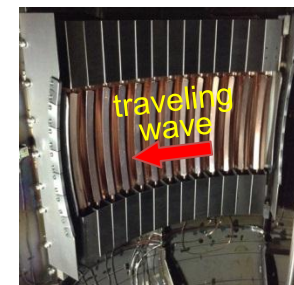
Non-inductive Plasma Start-up Experiments on the TST-2 Spherical Tokamak Using Waves in the Lower-Hybrid Frequency Range

Y. Takase for the TST-2 Group

- **Economically competitive tokamak reactor may be realized at low $A = R/a$ by eliminating the central solenoid**
→ **Objective: Demonstrate I_p ramp-up by LHW on ST**

- Three antennas were used:

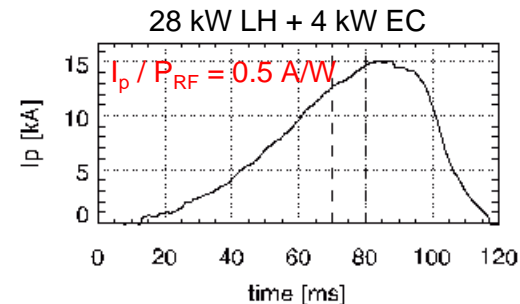
- Compline antenna
 - Nonlinear excitation of LHW
- Grill (dielectric-loaded WG array) antenna
 - Optimum $n_{||}$: 3-4
- CCC (capacitively-coupled compline) antenna
 - Highest η_{CD} achieved (sharp $n_{||}$ spectrum, good directivity)



CCC antenna

- Characteristics of LH driven plasma

- Pressure dominated by fast electrons
 - 3-fluid equilibrium being developed
 - Importance of E_r and flows
- Fast electrons are poorly confined at $I_p \sim 10$ kA
 - η_{CD} much smaller than in typical tokamak experiments
 - Due to poor orbit confinement of fast electrons
 - Expected to improve significantly at higher I_p and B_t (need power supply upgrade)



- Various diagnostics and analysis tools are being developed

- Wave diagnostics, HX profile, E_r flows, J profile, etc.

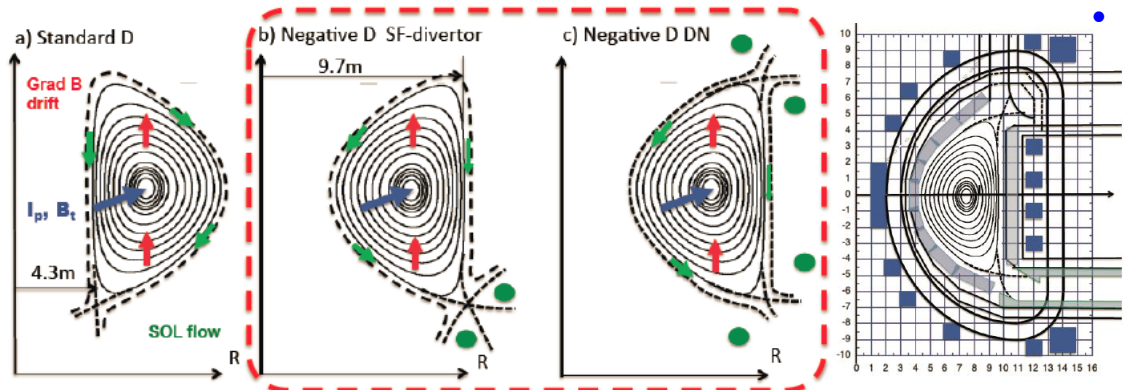
Innovative Confinement Concepts

15 papers

- ✓ Tokamaks with novel magnetic configurations
- ✓ Advances in Field Reversed Configurations
- ✓ Spherical Configurations other than tokamaks (HIT-SI)
- Advances in Spherical Tokamaks (TS4)
- ✓ New ideas/concepts for fusion reactors

Negative triangularity tokamak: stability limits and perspectives as fusion energy system

Power and particle control is an issue in D-shaped ($\delta > 0$) cross-section tokamak with H-mode optimized for core confinement



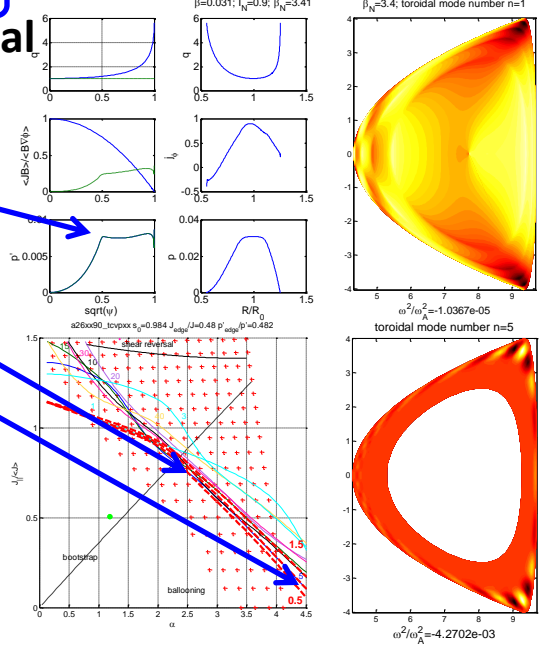
Assess negative D to solve power and particle exhaust problem!

- Edge stability \rightarrow different ELM regime (MHD stability)
- Geometry of power handling area \leftarrow larger R_{div}
- SOL flow \rightarrow slower, wider SOL
- Better confinement: $\delta < 0$ edge transport rather than core
- Technical merits: HFS ECCD, lower background magnetic field for internal PF coils, larger pumping conductance from divertor

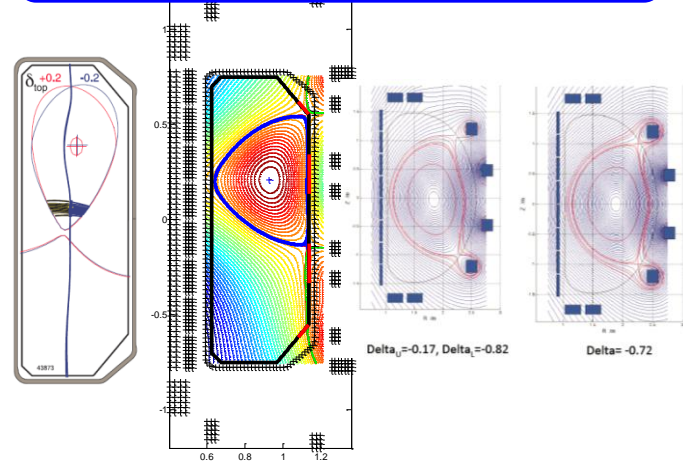
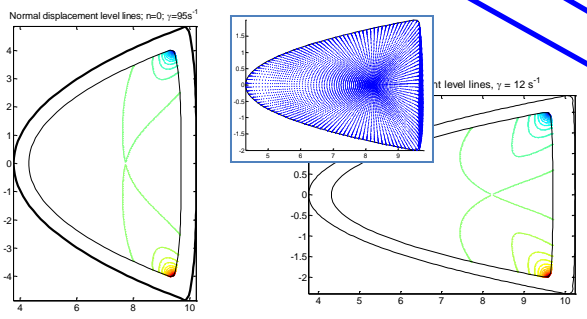
MHD stability

- Beta limit against $n=1$ external mode $\beta_N > 3$ for optimized profiles
- No 2nd stability access in the pedestal; high p' in the 1st
- $n=0$ stability to be mitigated

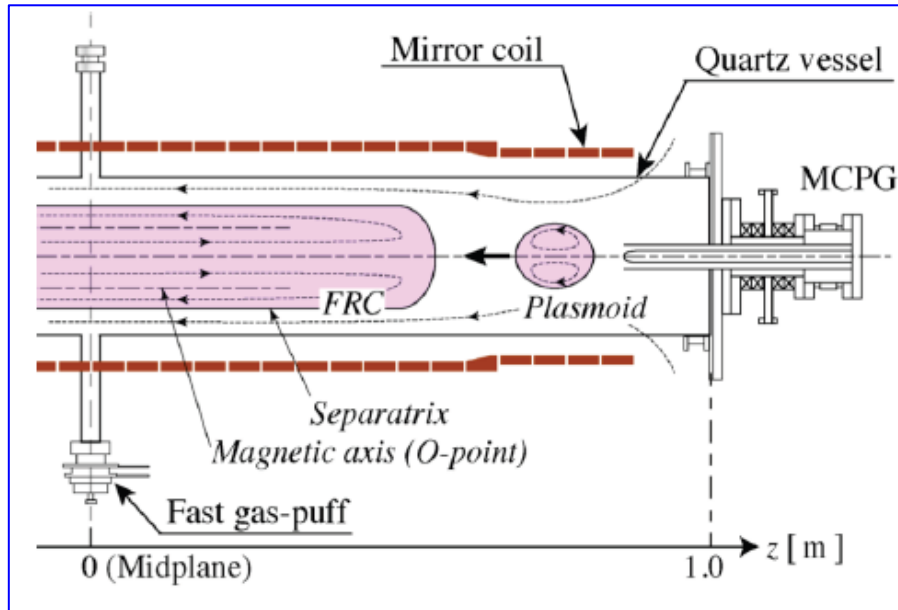
Positive shear $I_p=0.9$: $\beta_N < 3.2$



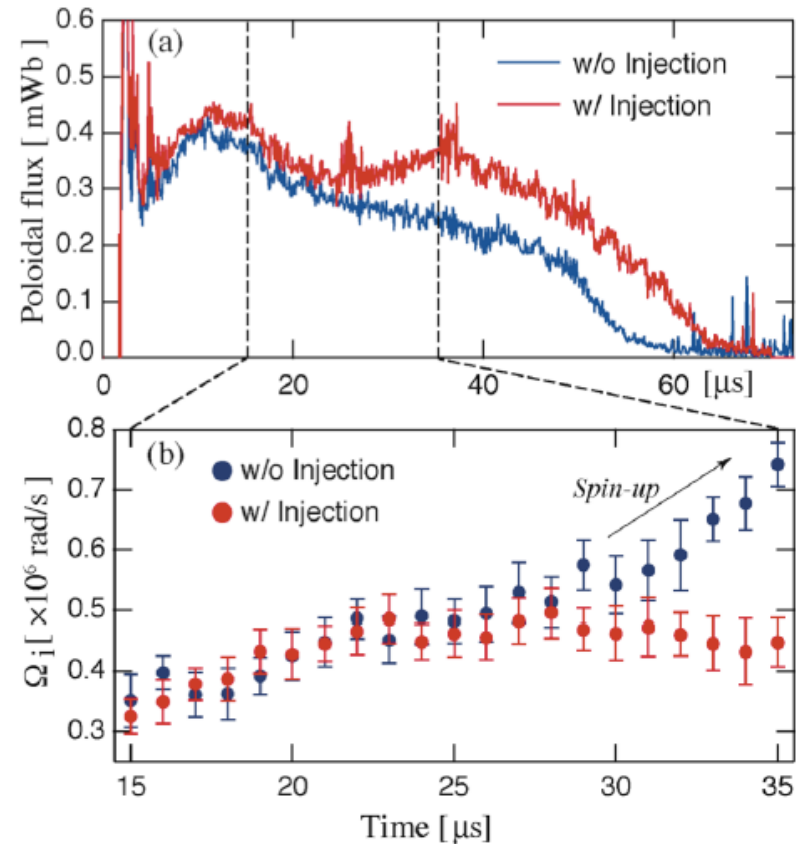
Experimental proposals: TCV, HL-2M, DIII-D



Control of Rotational Instability in FRC



- Toroidal spin-up in an FRC triggers a centrifugally- driven interchange-like mode $n = 2$.
- Suppression of Spontaneous Rotation in a FRC by Magnetized Plasmoid Injection in NUCTE device



ICC/P5-43, Asai

Spherical Configuration

- Significant progress on Current Drive in HIT-SI
- By increasing the frequency of the Imposed Dynamo Current Drive (IDCD) up to 68.5 kHz
- Toroidal currents of 90 kA and current gains of nearly 4, a spheromak record, have been achieved.
- dynamo current drive does not need plasma-generated fluctuations -a stable equilibrium with profile control can be sustained with imposed fluctuations
- Extrapolation to ITER - 80 kHz gives injector powers less than 10 MW and $\delta B/B \approx 10^{-4}$ indicating the effect on confinement may be acceptable.



ICC/P4-31, Victor

**1 Gwe Reactor Dynamak
Jarboe**

Concluding Remarks

EXS , EXW:

- **Focused international efforts on ITER relevant issues has considerably advanced our understanding on ELM physics and disruption phenomena**
- **Runaway mitigation system not yet firmly established - but there are promising leads that need to be followed**
- **Alternate ELM mitigation systems that do not require IVCs show considerable promise and may provide an attractive future option for ITER**
- **New ideas on disruption avoidance and control need validation on larger machines**

Concluding Remarks

ICC:

- **Heartening to see good scientific progress in alternatives to the tokamak/stellarator approach - e.g. Spheromaks, FRCs**
- **Exploration and development of such alternate schemes essential for improving our chances of early fusion power – we need to promote more new ideas**

**Exciting week - wealth of scientific results
- wonderful hospitality**

Thanks to our hosts and IAEA